Solid State Ionics 311 (2017) 127–131

Contents lists available at ScienceDirect

Solid State Ionics

journal homepage: www.elsevier.com/locate/ssi

Synchrotron X-ray studies of model SOFC cathodes, part II: Porous powder cathodes

Kee-Chul Chang[a], Brian Ingram[b], Jan Ilavsky[c], Shiwoo Lee[d,e], Paul Fuoss[a], Hoydoo You[a,*]

[a] Materials Science Division, Argonne National Laboratory, Argonne, IL 60439, United States
[b] Chemical Sciences and Engineering Division, Argonne National Laboratory, Argonne, IL 60439, United States
[c] X-ray Science Division, Argonne National Laboratory, Argonne, IL 60439, United States
[d] U.S. DOE, National Energy Technology Laboratory, Morgantown, WV 26507, United States
[e] AECOM, Morgantown, WV 26507, United States

ABSTRACT

Infiltrated $La_{0.6}Sr_{0.4}Co_{0.2}Fe_{0.8}O_{3-\delta}$ (LSCF) sintered porous powder cathodes for solid oxide fuel cells have been investigated by synchrotron ultra-small angle x-ray scattering (USAXS). We demonstrated that atomic layer deposition (ALD) is the method for a uniform coating and liquid-phase infiltration for growing nanoscale particles on the porous LSCF surfaces. The MnO infiltrate, grown by ALD, forms a conformal layer with a uniform thickness throughout the pores evidenced by USAXS thickness fringes. The $La_{0.6}Sr_{0.4}CoO_3$ (LSC) and $La_2Zr_2O_7$ (LZO) infiltrates, grown by liquid-phase infiltration, were found to form nanoscale particles on the surfaces of LSCF particles resulting in increased surface areas. Impedance measurements suggest that the catalytic property of LSC infiltrate, not the increased surface area of LZO, is important for increasing oxygen reduction activities.

1. Introduction

In solid oxide fuel cell (SOFC), mixed ionic and electronic conducting perovskite oxides such as $(La,Sr)MnO_{3-\delta}$ (LSM), $(La,Sr)CoO_{3-\delta}$ (LSC), and $La_{0.6}Sr_{0.4}Co_{0.2}Fe_{0.8}O_{3-\delta}$ (LSCF) are commonly used as cathode materials [1]. While LSM is a common cathode material for stability, significant efforts were made to search for cathode materials with a high ionic conductivity operable at lower temperatures and the cathode materials such as LSC [2], and its A-site variation were studied [3]. More recently, LSCF [4] is widely accepted as the cathode with a good compromise of high conductivity and stability to replace LSM [5]. To reduce the operating temperature, the oxygen reduction reaction (ORR) activity of the porous cathodes needs to be increased as the ORR overpotential represents the most significant internal loss [6,7]. A strategy for increasing the ORR activity is infiltrating [8] active materials to the sintered power cathodes, which will be the focus of this paper.

Ultra-Small Angle X-ray Scattering (USAXS) is one of the best matching x-ray techniques for *in situ* study of porous powder cathodes. The pore size distributions (from nanometer to microns) of SOFC cathodes have been shown to be well matched to the USAXS capabilities [9,10]. More importantly, USAXS is sensitive enough to characterize the infiltrate in addition to the LSCF backbone. There are other x-ray techniques for studying the correlation of microstructure with electrochemical performance such as x-ray micro-tomography [11,12]. This technique can produce ~10 nm resolution real space three-dimensional images over $\sim 10^3\ \mu m^3$ volume. It is non-destructive and allows imaging of the sample under operating conditions. It can also be combined with x-ray fluorescence for elemental sensitivity at the cost of worse imaging resolution. The main restriction of x-ray micro-tomography for *in situ* SOFC experiments is that the sample has to be ~10 μm thick in two dimensions, which complicates the setup of an *in situ* cell. Therefore, we utilize only USAXS technique for characterizing the infiltrates and LSCF backbone structures.

2. Experiment

2.1. Porous sample preparation

The main constraint in sample fabrication for USAXS is to make freestanding samples thin enough for x-ray transmission yet thick enough for sufficient scattering intensity. For use of x-ray energy above 16 keV the samples were made by a screen printing technique. Approximately 10 μm thick layers of cathodes and YSZ, schematically shown in Fig. 1, was printed on 0.3 mm thick $Al_2O_3(0001)$ or 0.5 mm thick MgO(001) single crystal substrate. The screen printed LSCF was

* Corresponding author.
E-mail address: hyou@anl.gov (H. You).

http://dx.doi.org/10.1016/j.ssi.2017.10.001
Received 7 August 2017; Received in revised form 30 September 2017; Accepted 3 October 2017
0167-2738/ Published by Elsevier B.V.

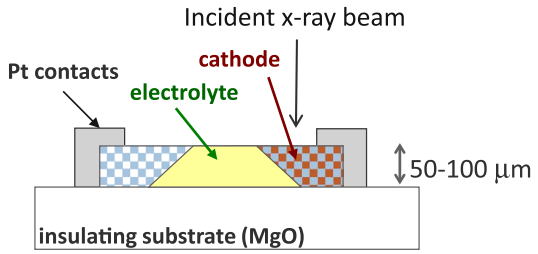

Fig. 1. Schematic illustration of the experimental setup for porous cathodes in a symmetric cell configuration operated in a half-cell configuration for a transmission geometry.

annealed at 1000 °C for ~1 h to burn out the polymers in the ink and to sinter the powders. YSZ was annealed at 1400 °C for use as an electrolyte in SOFC cell or 1200 °C just as a backbone structure of infiltrates, respectively. Because of the well-known solubility of YSZ and Al_2O_3 above ~1400 °C, some critical experiments were repeated with MgO substrates to ensure the results presented here are not affected by the formation of the solid solution. Even though the infiltrated cathodes are the main purpose, USAXS measurements from three different types of samples are used to investigate systematically: (i) LSCF on Al_2O_3 substrates to determine the ideal thickness for USAXS, (ii) a symmetric SOFC cell test structure on MgO, (iii) a LSCF infiltrated YSZ on MgO for *in situ* temperature processing measurements. The final samples were the LSCF porous powders infiltrated by MnO, using an atomic layer deposition (ALD) technique, and by LSC and $LaZrO_3$ (LZO), using a liquid-phase infiltration technique.

2.2. USAXS measurement

The small angle x-ray scattering (SAXS) technique [13,14] probes the average particle size, particle size distribution, and the surface-to-volume ratio at length scales of 1 to 100 nm. The length scale can be extended to ~1 μm in Ultra Small Angle X-ray Scattering (USAXS) [15] technique. We used the USAXS instrument at sector 15 (ChemMat CARS) at APS [16]. The instrument uses Bonse-Hart [17] double-crystal configuration for scattering vector ranges of $\sim 10^{-4}$ to $\sim 10\ Å^{-1}$, which are equivalent to the length sensitivity to ~10 μm to ~10 nm length scale. The double-crystal configuration uses a pair of multiple-bounce channel cut monochromator and analyzer, in order to increase the resolution and discriminate the diffraction from the intense main beam. It uses an undulator source for a dynamic intensity range of 10^8 to 10^9 depending on the configuration. We used x-ray energy of 16–18 keV for our experiments. Linkam TS1500 heater [18], equipped with sapphire windows and capable of heating to 1500 °C, was used for *in situ* heating experiments. The resulting USAXS data was analyzed using Irena small angle scattering analysis software suite [19].

3. Results and discussion

3.1. Porod's law and thickness fringes

In analyzing and understanding the x-ray reflectivity or small-angle scattering, it is convenient to write an equation for the scattering intensity from interfaces. Here we define an interface to be an elemental area whose electron density changes only in the normal direction. We call 'x-ray reflectivity' when the interfaces form an overall relatively well-defined flat surface and 'small-angle scattering' when the interfaces are complex and often convoluted. In both cases, x-rays scatter only from the interfaces. The interface scattering can be then written in two terms: [20]

$$I(q) = \sum_{n=1}^{N} \boldsymbol{V}_n^2(q) + 2\sum_{m<n}^{N} \boldsymbol{V}_m(q)\cdot\boldsymbol{V}_n(q)\cos(\varphi_m - \varphi_n) \quad (1)$$

where $\boldsymbol{V}_n(q)$ is a reflection amplitude from n^{th} interface, $\varphi_m - \varphi_n = qd$ is the phase difference associated with the distance between the layers. The first term represents the sum of scattering intensities from individual interfaces and the second term represents the interference between them. This derivation is essentially a Hendricks and Teller expansion [21] approach for the better known Ciccariello and Benedetti's oscillatory deviations [22,23], which can be obtained by angular average of Eq. (1).

The amplitude $V \approx \left(q_c/2q\right)^2$ with q_c being the critical angle of the interface that is proportional to the electron-density jump at the interface. This is a good approximation for USAXS from complex interfaces where the scattering can be approximated to a kinematic limit. The first term then behaves smoothly with a function q^{-4} following Porod's law. The second term behaves similarly except for the oscillatory term multiplied. For random layer thicknesses, the oscillatory terms are averaged and cancelled out. Then the overall scattering, the first term plus the second term, recovers the Porod's law. However, for a conformal roughness [20], where the thickness of the overlayer is uniform, the unique thickness fringe of the cosine term can ride on the Porod's law behavior.

3.2. MnO Infiltrate Grown by atomic layer deposition on LSCF

Infiltration techniques have been successful in improving catalytic activities [8]. While the liquid-phase infiltration has been successful, *e.g.*, LSM infiltration to LSCF cathodes [24], in improving the stability and catalytic activity, we explored a gas-phase infiltration, atomic layer deposition (ALD) technique, for better penetration of the infiltrates deep into the porous cathode materials. As the first step, we tested the ALD of MnO on LSCF thin film, epitaxially grown on $NdGaO_3$ (011) substrate by pulse laser deposition (PLD) [25]. The film was examined with x-ray reflectivity (XR) technique before the ALD, after the ALD, and after annealing the ALD layer.

The thickness of LSCF films was ~10 nm thick pre-determined by a XR measurement and that of MnO was nominally ~5 nm. Fig. 2(a) shows the evolution of the XR on this sample annealed to 700 °C. The XR at room temperature (RT) shows a fringe of $\sim 0.05\ Å^{-1}$. This corresponds to the overall thickness of ~15 nm as expected. Annealing it to 500 °C makes the XR change significantly. However, there is not much change in the average fringe width, therefore, the overall thickness. Analysis of the data indicates that the major change occurs on the surface roughness. The XR decreases at large $Q > 0.3\ Å^{-1}$ by annealing at 500 °C. This occurs because the roughness of the MnO/LSCF interface increases from 2 to 5 Å. The roughness of MnO surface, which was initially measured at ~10 Å at RT, appears decreasing to ~5 Å by annealing at 500 °C. This can happen when the MnO layer is partially conformal to the MnO/LSCF interface. The total roughness remains ~10 Å as before because the roughness of the underlying MnO/LSCF layer is already at 5 Å. This result suggests that the initially grown ALD layer undergoes conformal layering at 500 °C, *i.e.*, forming a rather uniform MnO layer following the undulation of LSCF surface.

With the evidence of the conformal ALD growth on the film cathodes, we tested the feasibility with the porous samples: ALD deposition of MnO on sintered porous YSZ backbone. We prepared samples with nominally 10 and 50 nm thick MnO layers. However, the preliminary USAXS pattern from the 10 nm thick sample was almost indistinguishable from that obtained from the YSZ backbone. Therefore, we focus on the 50 nm thick MnO infiltrate layer annealed at from RT to 800 °C. The *ex situ* USAXS data taken at several temperatures are compared to that of the backbone in Fig. 2(b). The ALD layer results in the fringes at high Q values of USAXS data. The fringes can be seen more clearly by dividing the data by the backbone data and they are shown in the inset of Fig. 2(b).

Using the oscillatory term of Eq. (1), $\cos(2\pi Qd)$ with $q = 2\pi Q$, we can estimate the thickness of MnO infiltrate. Since the ALD process and the annealing to 600 °C are not expected to increase YSZ particle sizes significantly, we can estimate the average MnO layer thickness from the